Bayesian inference for transportation origin-destination matrices: the Poisson-inverse Gaussian and other Poisson mixtures

Konstantinos Perrakis[*], Dimitris Karlis[†], Mario Cools[‡]
and Davy Janssens[*]

Abstract

In this paper we present Poisson mixture approaches for origin-destination (OD) modeling in transportation analysis. We introduce covariate-based models which incorporate different transport modeling phases and also allow for direct probabilistic inference on link traffic based on Bayesian predictions. Emphasis is placed on the Poisson-inverse Gaussian as an alternative to the commonly-used Poisson-gamma and Poisson-lognormal models. We present a first full Bayesian formulation and demonstrate that the Poisson-inverse Gaussian is particularly suited for OD analysis due to desirable marginal and hierarchical properties. In addition, the integrated nested Laplace approximation (INLA) is considered as an alternative to Markov chain Monte Carlo and the two methodologies are compared under specific modeling assumptions. The case study is based on 2001 Belgian census data and focuses on a large, sparsely-distributed OD matrix containing trip information for 308 Flemish municipalities.

Keywords: Hierarchical Bayesian modeling; INLA; OD matrix; overdispersion; Poisson mixtures

1 Introduction

In transportation analysis the *travel demand* within a geographical area, dividable into a given number of non-overlapping zones, is summarized by an OD matrix which contains the *trips* or *flows* that have occurred from each zone of that area to every other zone. Consider an area which can be divided into m zones and let T_{od} denote the flows from

---

[*]Transportation Research Institute, Hasselt University, Belgium (1st author now in: Department of Hygiene, Epidemiology and Medical Statistics, Medical School, University of Athens, Greece); kperrakis@med.uoa.gr, davy.janssens@uhasselt.be

[†]Department of Statistics, Athens University of Economics and Business, Greece; karlis@aueb.gr

[‡]LEMA, University of Liège, Belgium; mario.cools@ulg.ac.be

zone of *origin o* to zone of *destination d*, where $o, d = 1, 2, ..., m$. The OD matrix $\mathbf{T}$, is then

$$\mathbf{T} = \begin{bmatrix} T_{11} & T_{12} & \ldots & T_{1m} \\ T_{21} & T_{22} & \ldots & T_{2m} \\ \vdots & \vdots & \ddots & \vdots \\ T_{m1} & T_{m2} & \ldots & T_{mm} \end{bmatrix}.$$

The elements T_{od}, for $o \neq d$, correspond to *inter-zonal* flows, whereas the elements across the main diagonal T_{oo} correspond to *intra-zonal* flows. The marginal totals $T_{o\bullet} = \sum_d T_{od}$ and $T_{\bullet d} = \sum_o T_{od}$ are commonly referred to as *trip-productions* and *trip-attractions*, respectively. In lexicographical order the matrix $\mathbf{T}$ can be represented as $\mathbf{y} = (y_1, y_2, \ldots, y_n)^T$ $\equiv (T_{11}, T_{12}, \ldots, T_{mm})^T$ with $n = m^2$.

The inferential scope in OD modeling depends on several defining aspects such as spatial resolution, time resolution and classification by trip-purpose. In addition, OD modeling is itself part of a larger inferential framework. Specifically, the traditional transportation modeling framework consists of a sequence of 4 modeling steps, namely (a) trip-generation, (b) trip-distribution, (c) modal-split and (d) traffic-assignment. Trip-generation models are typically regression or cross-classification models which relate trip-productions and trip-attractions to socio-economic, location and land-use variables. Trip-distribution models balance trip-productions and trip-attractions, and distribute the trips to the cells of an OD matrix usually by using supplementary prior information in the form of an outdated OD matrix. Commonly used trip-distribution models include gravity and direct-demand models. The subsequent step of modal-split entails disaggregating the OD matrix with respect to mode choice. Finally, traffic-assignment involves allocating the $n - m$ inter-zonal flows on a corresponding transport network consisting of all the available links which define the possible routes from zone of origin o to zone of destination d, for $o, d = 1, 2, ..., m$ and $o \neq d$. Interested readers are referred to Ortúzar and Willumsen (2001) for four-step modeling and to Thomas (1991) for traffic-assignment.

In general, the four-step procedure remains widely accepted by transportation planners, so that OD modeling up to the present is mainly based on trip-generation and trip-distribution principles. A first modern Bayesian approach to trip-distribution, based on the gravity model, is discussed in West (1994). It is also worth noting that a different approach for OD estimation relies on information from link traffic data where the traffic-assingment problem is actually inverted; see e.g. Tebaldi and West (1998) and Hazelton (2010) for Bayesian methods. The methodological framework is quite different under this approach and it is actually part of a broader literature on network tomography (e.g. Medina et al., 2002). In this study we extend the methodology presented in Perrakis et al. (2012a) for OD modeling based on census data and Perrakis et al. (2012b) for traffic-assignment inference through Bayesian predictions. Additional references concerning OD estimation from travel-surveys and/or link traffic can be found in Perrakis et al. (2012a).

In particular, we investigate the performance of three Poisson mixture models, namely the Poisson-gamma (PG), Poisson-lognormal (PLN) and Poisson-inverse Gaussian (PIG) models. The PG model is the most commonly used and well established model within the

family of Poisson mixtures, while the PLN model remains up to present the predominant alternative. The PIG model is the less known and less used model among the three, especially within the Bayesian framework. We present a first full Bayesian treatment of the PIG model and demonstrate that it has desirable properties both in its marginal and in its hierarchical forms. In addition, we consider the integrated nested Laplace approximation (INLA) framework (Rue et al., 2009) as a potentially efficient alternative to Markov chain Monte Carlo methods for the PG and PLN models. The case study focuses on a large-scale OD matrix, derived from the 2001 Belgian census study, containing trip-information for 308 municipalities in the region of Flanders.

The paper is organized as follows. Literature review and Bayesian formulations for the three models in question are provided in section 2. The OD matrix, the transport network of Flanders and the selection of explanatory variables are described in section 3. Results are presented in section 4. The paper ends with conclusions and considerations of future research in section 5.

2 Poisson mixture models

With Poisson mixture models we assume that the OD flows y_i are i.i.d. Poisson realizations and that the rate of the Poisson distribution is $\lambda_i = \mu_i u_i$ for $i = 1, 2, ..., n$. The rate λ_i is split in two parts; μ_i is the part which is related to the vector of $p + 1$ unknown parameters $\boldsymbol{\beta} = (\beta_0, \beta_1, ..., \beta_p)^T$ and the set of explanatory variables $\mathbf{x}_i = (1, x_{i1}, ..., x_{ip})^T$ through the log-link function $\log \mu_i = \boldsymbol{\beta}^T \mathbf{x}_i$, and u_i is a random component – interpreted as a multiplicative random effect accounting for heterogeneity – which is attributed with a density $g_1(u_i)$. The Poisson mixture modeling formulation is summarized as follows

$$y_i \sim Pois(\lambda_i), \text{ with } \lambda_i = \mu_i u_i \text{ and}$$
$$\mu_i = \exp(\boldsymbol{\beta}^T \mathbf{x}_i),$$
$$u_i \sim g_1(u_i) \text{ and } E(u_i) = 1.$$

The density g_1 is known as the mixing density and can be continuous, discrete or even a finite support distribution. The constrain on the expected value of the random component u_i ensures that the model is scale-identifiable. Poisson mixtures are employed as overdispersed alternatives to the simple Poisson model which arises when the mixing density becomes degenerate. Alternatively, from a GLMM perspective the above model can be expressed as

$$y_i \sim Pois(\lambda_i) \text{ with } \log \lambda_i = \boldsymbol{\beta}^T \mathbf{x}_i + \varepsilon_i,$$
$$\varepsilon_i \sim g_2(\varepsilon_i) \text{ and } E(\varepsilon_i) = 0,$$

where ε_i is an additive random error term. Here the constraint on the expected value ensures location-identifiability. The two formulations are equivalent, however the intercepts and the interpretations of marginal means are different due to the identifiability constraints (Lee and Nelder, 2004). The Poisson likelihood is the conditional likelihood given the unobserved random effect vector $\mathbf{u} = (u_1, u_2, ..., u_n)^T$. Integration over $\mathbf{u}$ results to the marginal sampling likelihood, i.e. $p(\mathbf{y}|\boldsymbol{\mu}) = \int p(\mathbf{y}|\boldsymbol{\mu}, \mathbf{u}) g_1(\mathbf{u}) d\mathbf{u}$. Frequentist inference

usually focuses on the marginal structure under maximum-likelihood (ML), restricted-ML, quasi-likelihood and pseudo-likelihood estimation procedures.

When the mixing density g_1 is a gamma distribution, we have the PG model which is the most frequently used Poisson mixture model due to the property that the resulting marginal likelihood is a negative binomial distribution. Properties and estimation procedures for negative binomial regression can be found in Lawless (1987). The PG model is also included in the family of hierarchical generalized linear models (HGLM's) introduced by Lee and Nelder (1996) who provide ML estimates for regression parameters as well as random effects based on the hierarchical likelihood (h-likelihood). The PLN model arises when g_1 is a lognormal distribution. The resulting marginal distribution of this model, known simply as Poisson-lognormal (Shaban, 1988), does not have a closed form expression and thus numerical integration is needed for marginal estimation. Nevertheless, the PLN model is regularly used in practice due to its distinct historical development as a GLMM for count data based on the assumption that g_2 is a normal distribution (Breslow 1984). Estimation of the model through Gaussian quadrature and the EM algorithm is handled in Aitkin (1996). An inverse Gaussian (IG) density for g_1 results in the PIG model which leads to a Poisson-inverse Gaussian marginal density. This distribution, unlike the Poisson-lognormal case, does have a closed form expression. The PIG model was first presented by Holla (1967). Information on ML estimation can be found in Dean et al. (1989) and in the references therein. The PIG model has been used in the actuarial science (Willmot, 1987; Carlson, 2002) and in linguistics where the zero-truncated marginal form is of particular interest (e.g. Puig et al., 2009).

A first consideration of all three models is presented in Chen and Ahn (1996). Later, Karlis (2001) provided a generally applicable EM algorithm for Poisson mixtures and compared the three models on a real dataset. In Boucher and Denuit (2006), the performance of the three models is investigated from a random-effects versus fixed-effects perspective on motor insurance claims. Finally, in Nikoloulopoulos and Karlis (2008) the models are compared with respect to distributional properties such as skewness and kurtosis under simulation experiments. This study illustrates some theoretical expectations, namely that the PLN and PIG models allow for longer right tails and are thus more appropriate than the PG model for modeling highly positive-skewed data.

From a Bayesian perspective, Poisson mixtures have a natural interpretation as hierarchical or multilevel models where the mixing distribution is considered as a first-level prior of which the parameters are assigned with a second-level prior or hyperprior. With respect to the equivalence between the multiplicative and additive forms, it is the choice of hyperprior which affects inferences about the intercept, depending upon whether the $E(u_i) = 1$ or $E(\varepsilon_i) = 0$ constraint is imposed through the hyperprior. Bayesian applications of negative binomial modeling as well as hierarchical PG and PLN modeling can be found in Ntzoufras (2009) and in the references therein. Bayesian literature on PIG modeling is limited to the study of Font et al. (2013), which emphasizes on a marginal, zero-truncated form of the model specifically suited for linguistic analysis.

In what follows, we present the hierarchical and marginal forms and properties of the three models, with emphasis placed on the PIG. Markov chain Monte Carlo (MCMC)

4

sampling is based on a posterior factorization which is not common, but is particularly convenient in our context given the large data size. Specifically, if we denote by ω the hyper-parameter of the mixing prior of $\mathbf{u}$, then the joint posterior is $p(\boldsymbol{\mu}, \mathbf{u}, \omega|\mathbf{y}) = p(\mathbf{u}|\boldsymbol{\mu}, \omega, \mathbf{y})p(\boldsymbol{\mu}, \omega|\mathbf{y})$. Thus, for hierarchical inference one can use the marginal likelihood for sampling from $p(\boldsymbol{\mu}, \omega|\mathbf{y})$ and generate $\mathbf{u}$ subsequently from $p(\mathbf{u}|\boldsymbol{\mu}, \omega, \mathbf{y})$. As illustrated next, this is straightforward for the PG and PIG models.

2.1   The PG model

For the PG model we make the following likelihood and prior assumptions;

$$
\begin{aligned}
&y_i|\boldsymbol{\beta}, u_i \sim Poisson(\exp(\boldsymbol{\beta}^T\mathbf{x}_i)u_i), \\
&\boldsymbol{\beta} \sim \mathbf{N}_{p+1}(\mathbf{0}, \boldsymbol{\Sigma}_{\boldsymbol{\beta}}) \text{ with } \boldsymbol{\Sigma}_{\boldsymbol{\beta}} = n(\mathbf{X}^{'}\mathbf{X})^{-1}, \\
&u_i \sim Gamma(\theta, \theta) \text{ and} \\
&\theta \sim Gamma(a, a) \text{ with } a = 10^{-3}.
\end{aligned}
$$

For the multivariate normal prior of the regression parameters we adopt the g-prior structure (Zellner, 1986), analogue to the benchmark prior discussed in Fernández et al. (2001) for normal linear models. The same unit-information multivariate prior is also adopted for the PLN and PIG models. The gamma prior for u_i is defined in terms of shape and rate parameters which both equal θ, so that $E(u_i) = 1$ and $Var(u_i) = \theta^{-1}$. The gamma hyperprior for dispersion parameter θ, with shape and rate equal to 0.001, is a commonly used diffuse prior (Ntzoufras, 2009). The joint posterior distribution of all parameters is $p(\boldsymbol{\beta}, \mathbf{u}, \theta|\mathbf{y}) \propto p(\mathbf{y}|\boldsymbol{\beta}, \mathbf{u})p(\boldsymbol{\beta})p(\mathbf{u}|\theta)p(\theta)$. The only full conditional which has a known form is that of the random effects which is a gamma distribution, namely $u_i|\boldsymbol{\beta}, \theta, y_i \sim Gamma(y_i + \theta, \mu_i + \theta)$ (Gelman and Hill, 2006). Therefore, MCMC for the hierarchical model would require a Metropolis-within-Gibbs type of algorithm with Metropolis steps for the joint conditional of $\boldsymbol{\beta}, \theta|\mathbf{u}, \mathbf{y}$ or for the conditionals of $\boldsymbol{\beta}|\mathbf{u}, \mathbf{y}$ and $\theta|\mathbf{u}, \mathbf{y}$. Alternatively, adaptive rejection sampling can also be used.

Integration over $\mathbf{u}$ leads to a negative binomial marginal likelihood, i.e. $y_i|\boldsymbol{\beta}, \theta \sim NB(\exp(\boldsymbol{\beta}^T\mathbf{x}_i), \theta)$. Under this parameterization the marginal mean and variance are given by $E(\mathbf{y}|\boldsymbol{\beta}) = \exp(\mathbf{X}\boldsymbol{\beta})$ and $Var(\mathbf{y}|\boldsymbol{\beta}, \theta) = \exp(\mathbf{X}\boldsymbol{\beta}) + \exp(\mathbf{X}\boldsymbol{\beta})^2\theta^{-1}$, with the variance being a quadratic function of the mean. The posterior distribution now is $p(\boldsymbol{\beta}, \theta|\mathbf{y}) \propto p(\mathbf{y}|\boldsymbol{\beta}, \theta)p(\boldsymbol{\beta})p(\theta)$, which leads to expression

$$
\begin{aligned}
p(\boldsymbol{\beta}, \theta|\mathbf{y}) \propto \exp\left(\mathbf{y}^T\mathbf{X}\boldsymbol{\beta} - \frac{1}{2}\boldsymbol{\beta}^T\boldsymbol{\Sigma}_{\boldsymbol{\beta}}^{-1}\boldsymbol{\beta} - a\theta\right)\theta^{n\theta+a}\Gamma(\theta)^{-n} \\
\times \prod_i \left[\Gamma(y_i + \theta)\left(\exp(\boldsymbol{\beta}^T\mathbf{x}_i) + \theta\right)^{-(y_i+\theta)}\right].
\end{aligned} \tag{1}
$$

The Metropolis-Hastings (M-H) algorithm is used to sample from the joint posterior of $\boldsymbol{\beta}, \theta|\mathbf{y}$. Once M posterior draws of $\boldsymbol{\beta}$ and θ are available, predictive inference from the hierarchical structure of the model is straightforward; we generate first $\mathbf{u}^{(m)} \sim Gamma(\mathbf{y} + \theta^{(m)}, \exp(\mathbf{X}\boldsymbol{\beta}^{(m)}) + \theta^{(m)})$ and then $\mathbf{y}^{pred(m)} \sim Poisson(\exp(\mathbf{X}\boldsymbol{\beta}^{(m)})\mathbf{u}^{(m)})$ for

$m = 1, 2, ..., M$. As shown in sections 4.4 and 4.5, predictions are used in posterior predictive checks and also for quantifying input-uncertainty in deterministic traffic-assignment modeling.

It is worth noting that recent developments (Martins and Rue, 2013) extend the initial INLA framework (Rue et al., 2009) to applications on near-Gaussian latent models. Therefore, we also consider INLA as an alternative to MCMC for the PG model; a comparison is presented in Section 4.1.

2.2 The PLN model

The assumptions are the following;

$$y_i|\boldsymbol{\beta}, u_i \sim Poisson(\exp(\boldsymbol{\beta}^T\mathbf{x}_i)u_i),$$
$$\boldsymbol{\beta} \sim \mathbf{N}_{p+1}(\mathbf{0}, \boldsymbol{\Sigma_\beta}) \text{ with } \boldsymbol{\Sigma_\beta} = n(\mathbf{X}^T\mathbf{X})^{-1},$$
$$u_i \sim LN(-\sigma^2/2, \sigma^2) \text{ and}$$
$$\sigma^2 \sim InvGamma(a, a) \text{ with } a = 10^{-3}.$$

Following the formulation of Lee and Nelder (2004) for scale identifiability, the prior distribution of u_i has location parameter equal to $-\sigma^2/2$ and scale σ^2, and so $E(u_i) = 1$ and $Var(u_i) = e^{\sigma^2} - 1$. The inverse gamma hyperprior for σ^2 is the common option for this model (Ntzoufras, 2009); for $a = 10^{-3}$ the distribution of σ^{-2} is a diffuse gamma. The joint posterior distribution is $p(\boldsymbol{\beta}, \mathbf{u}, \sigma^2|\mathbf{y}) \propto p(\mathbf{y}|\boldsymbol{\beta}, \mathbf{u})p(\boldsymbol{\beta})p(\mathbf{u}|\sigma^2)p(\sigma^2)$. In this case, none of the full conditional distributions are of known form. MCMC sampling for the hierarchical PLN model is in general more convenient in its GLMM form where the full conditional distribution of σ^2 is again an inverse gamma distribution, namely $\sigma^2|\mathbf{u}, \mathbf{y} \sim InvGamma(a + n/2, a + \sum_i (\log u_i)^2/2)$. Thus, in the additive case sampling from the conditionals of $\boldsymbol{\beta}$ and $\mathbf{u}$ is possible with Metropolis steps or rejection-sampling. Note that in the GLMM form the corresponding prior for u_i must be specified as $LN(0, \sigma^2)$.

In the PLN model the marginal likelihood $p(\mathbf{y}|\boldsymbol{\beta}, \sigma^2)$ is not known analytically, nevertheless the mean and variance of the PLN distribution are available and given by $E(\mathbf{y}|\boldsymbol{\beta}) = \exp(\mathbf{X}\boldsymbol{\beta})$ and $Var(\mathbf{y}|\boldsymbol{\beta}, \sigma^2) = \exp(\mathbf{X}\boldsymbol{\beta}) + \exp(\mathbf{X}\boldsymbol{\beta})^2(\exp(\sigma^2) - 1)$. As with the PG model, the variance is a quadratic function of the mean. The joint posterior density is $p(\boldsymbol{\beta}, \sigma^2|\mathbf{y}) \propto p(\mathbf{y}|\boldsymbol{\beta}, \sigma^2)p(\boldsymbol{\beta})p(\sigma^2)$, namely

$$
\begin{aligned}
p(\boldsymbol{\beta}, \sigma^2|\mathbf{y}) \propto \prod_i &\left[\int \exp\left(y_i\boldsymbol{\beta}^T\mathbf{x}_i - \exp\boldsymbol{\beta}^T\mathbf{x}_i u_i - \frac{(\log u_i + \sigma^2/2)^2}{2\sigma^2} \right) u_i^{y_i-1} du_i \right] \\
&\times \exp\left(-\frac{1}{2}\boldsymbol{\beta}^T\boldsymbol{\Sigma_\beta}^{-1}\boldsymbol{\beta} - a/\sigma^2 \right) \left(\sigma^2\right)^{-(n/2+a+1)}.
\end{aligned}
\tag{2}
$$

We employ M-H simulation in order to sample from the joint posterior density of $\boldsymbol{\beta}$ and σ^2. The integral appearing in the un-normalized posterior can be evaluated through numerical integration, e.g. with Gauss-Hermite quadrature which is also frequently employed in frequentist practice for marginal estimation. Another alternative examined in this study

is Monte Carlo (MC) integration from the lognormal prior of the random effect vector $\mathbf{u}$ within the Metropolis kernel. That is, for a given M-H iteration t and draws $\boldsymbol{\beta}^{(t)}, \sigma^{2(t)}$, the above integral can be evaluated by generating first L draws $\{u_i^{(t,l)}, \; l = 1, 2, ..., L\}$ from $u_i^{(t,l)} \sim LN(-\sigma^{2(t)}/2, \sigma^{2(t)})$ and then by calculating the marginal probability as $p(y_i|\boldsymbol{\beta}^{(t)}, \sigma^{2(t)}) = L^{-1} \sum_l p(y_i|\boldsymbol{\beta}^{(t)}, u_i^{(t,l)})$.

A potentially efficient alternative to MCMC approaches for the PLN model is the INLA framework introduced in Rue et al. (2009). The INLA approach covers the family of Gaussian Markov random fields (GMRF) models and is based on efficient approximating schemes for the marginal posterior distributions. The PLN model is included in the family of GMRF models as the random effects are normally distributed on additive scale. In Section 4.1 we compare INLA to MCMC.

2.3   The PIG model

For the hierarchical PIG we adopt the following assumptions;

$$y_i|\boldsymbol{\beta}, u_i \sim Poisson(\exp(\boldsymbol{\beta}^T \mathbf{x}_i)u_i),$$
$$\boldsymbol{\beta} \sim \mathbf{N}_{p+1}(\mathbf{0}, \boldsymbol{\Sigma_\beta}) \text{ with } \boldsymbol{\Sigma_\beta} = n(\mathbf{X}^T\mathbf{X})^{-1},$$
$$u_i \sim IG(1, \zeta) \text{ and}$$
$$\zeta \sim Gamma(a, a) \text{ with } a = 10^{-3}.$$

The initial parameterization of Holla (1967) is used for the IG prior, with mean μ and shape ζ, specifically

$$p(u_i|\mu, \zeta) = \left(\frac{\zeta}{2\pi u_i^3}\right)^{1/2} \exp\left(-\frac{\zeta(u_i - \mu)^2}{2\mu^2 u_i}\right). \tag{3}$$

For $\mu = 1$ we have that a-priori $E(u_i) = 1$ and $Var(u_i) = \zeta^{-1}$. The IG distribution is a special case of the three parameter generalized inverse Gaussian (GIG) distribution which is generally conjugate to the family of exponential distributionsis and is studied in detail in Jorgensen (1982). The p.d.f. of a $GIG(\lambda, \psi, \chi)$ distribution with parameters $\lambda \in$ R, $\chi, \psi > 0$ is given by

$$f(x) = \frac{(\psi/\chi)^{\lambda/2}}{2K_\lambda(\sqrt{\psi\chi})} x^{\lambda-1} \exp\left[-\frac{1}{2}\left(\psi x + \chi x^{-1}\right)\right], \tag{4}$$

where K_λ is the modified Bessel function of the third kind with order λ. The IG distribution arises for $\lambda = -1/2$. Interestingly, the gamma distribution is also a special case of the GIG distribution for $\chi = 0$. For shape parameter ζ we adopt the usual gamma hyperprior, similarly to the PG model. The posterior distribution now is $p(\boldsymbol{\beta}, \mathbf{u}, \zeta|\mathbf{y}) \propto p(\mathbf{y}|\boldsymbol{\beta}, \mathbf{u})p(\boldsymbol{\beta})p(\mathbf{u}|\zeta)p(\zeta)$ and it can be easily shown that the full conditionals of $\mathbf{u}$ and ζ are known distributions, namely $u_i|\boldsymbol{\beta}, \zeta \sim GIG(y_i - 1/2, 2\exp(\boldsymbol{\beta}^T\mathbf{x}_i) + \zeta, \zeta)$ and $\zeta|\mathbf{u} \sim Gamma(a + n/2, a + \sum_i (u_i - 1)^2/2u_i)$. Athreya (1986) was the first to notice the specific conjugate relationship between the IG and Poisson distribution; see also Karlis

(2001). Regarding simulation from the GIG distribution, random generators are readily available (e.g. Dagpunar, 1988). Thus, the hierarchical PIG model is actually simpler in terms of MCMC in comparison to the PG and PLN models, since all that is needed is a M-H step or rejection-sampling algorithm for the conditional of $\boldsymbol{\beta}$.

Marginally we have that $y_i|\boldsymbol{\beta}, \zeta \sim PIG(\exp(\boldsymbol{\beta}^T\mathbf{x}_i), \zeta)$ for $i = 1, 2, ..., n$ with p.d.f. given by

$$
\begin{aligned}
p(y_i|\boldsymbol{\beta}, \zeta) =& K_{y_i-1/2}\left(\sqrt{2\zeta\phi(\mathbf{x}_i)}\right)\left(\frac{2\zeta}{\pi}\right)^{1/2}\frac{\exp\left(\zeta/\exp(\boldsymbol{\beta}^T\mathbf{x}_i)\right)}{y_i!} \\
&\times \left(2\phi(\mathbf{x}_i)\zeta^{-1}\right)^{1/2(y_i-1/2)},
\end{aligned} \tag{5}
$$

where

$$
\phi(\mathbf{x}_i) = \left(1 + \frac{\zeta}{2\exp(\boldsymbol{\beta}^T\mathbf{x}_i)}\right). \tag{6}
$$

The marginal mean and variance are $E(\mathbf{y}|\boldsymbol{\beta}) = \exp(\mathbf{X}\boldsymbol{\beta})$ and $Var(\mathbf{y}|\boldsymbol{\beta}, \zeta) = \exp(\mathbf{X}\boldsymbol{\beta}) + (\exp(\mathbf{X}\boldsymbol{\beta}))^3\zeta^{-1}$. The variance is thus a cubic function of the mean in the PIG model, allowing for greater overdispersion. The posterior distribution $p(\boldsymbol{\beta}, \zeta|\mathbf{y}) \propto p(\mathbf{y}|\boldsymbol{\beta}, \zeta)p(\boldsymbol{\beta})p(\zeta)$ can be expressed as

$$
\begin{aligned}
p(\boldsymbol{\beta}, \zeta|\mathbf{y}) \propto& \prod_i \left[K_{y_i-1/2}\left(\sqrt{2\zeta\phi(\mathbf{x}_i)}\right)\exp\left(\zeta/\exp\left(\boldsymbol{\beta}^T\mathbf{x}_i\right)\right)\left(2\phi(\mathbf{x}_i)\zeta^{-1}\right)^{1/2(y_i-1/2)}\right] \\
&\times \exp\left(-\frac{1}{2}\boldsymbol{\beta}^T\boldsymbol{\Sigma}_{\boldsymbol{\beta}}^{-1}\boldsymbol{\beta} - a\zeta\right)\zeta^{n/2+a-1}.
\end{aligned} \tag{7}
$$

Samples from the posterior of $\boldsymbol{\beta}$ and ζ can be obtained through M-H simulation from the joint posterior. As with the PG model, when M posterior draws of $\boldsymbol{\beta}$ and ζ are available, predictive inference from the hierarchical structure of the PIG model is possible by generating first $\mathbf{u}^{(m)} \sim GIG(\mathbf{y} - 1/2, 2\exp(\mathbf{X}\boldsymbol{\beta}^{(m)}) + \zeta^{(m)}, \zeta^{(m)})$ and then $\mathbf{y}^{pred(m)} \sim Poisson(\exp(\mathbf{X}\boldsymbol{\beta}^{(m)})\mathbf{u}^{(m)})$ for $m = 1, 2, ..., M$.

3 Data

3.1 The OD matrix and the transport network of Flanders

The OD matrix was derived from the 2001 Belgian census study and contains information about the departure and arrival locations for work and school related trips of the approximately 10 million Belgian residents. The recorded work/school trips refer to a normal weekday for all possible travel modes and are one-directional, from zone of origin to zone of destination. The study area is not the entire country of Belgium, but the northern, Dutch-speaking region of Flanders which roughly accounts for 60% of the total population and 44% of the country's surface area. From an administrative viewpoint Flanders is divided into 5 provinces, 22 arrondissements, 52 districts, 103 cantons and 308 municipalities. Our analysis is implemented on the municipal level at which the OD matrix contains 94864 cells.
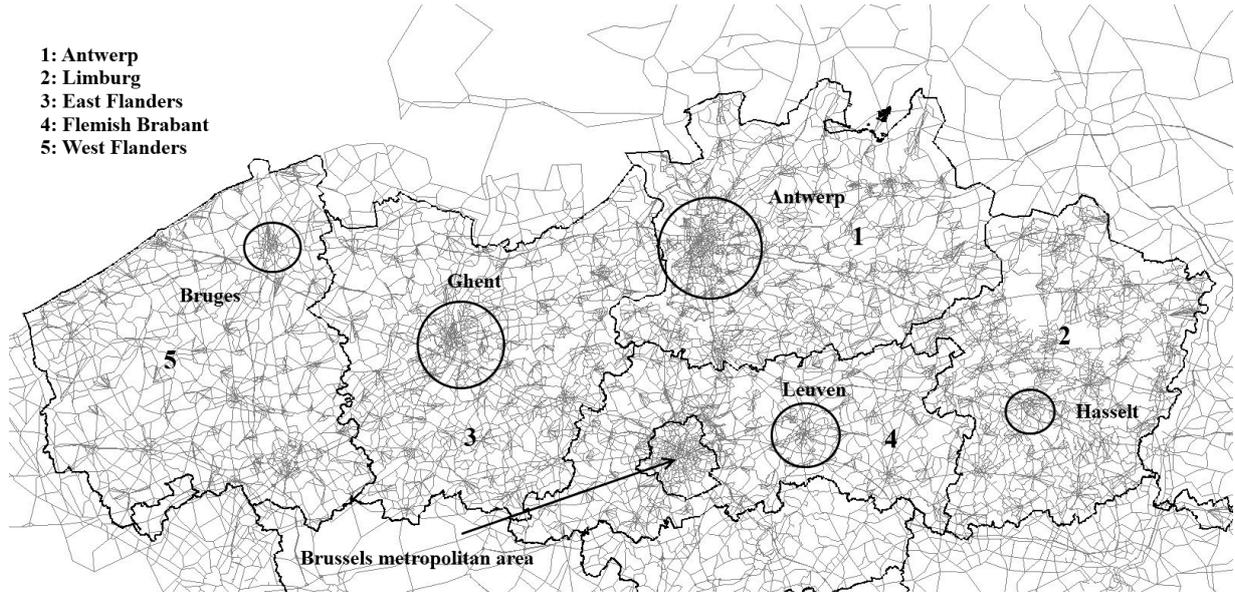
Figure 1: The road network of Flanders and the 5 Flemish provinces of Antwerp, Limburg, East Flanders, Flemish Brabant and West Flanders with corresponding capitals; Antwerp, Hasselt, Ghent, Leuven and Bruges.

The OD flows on municipality zonal level are sparsely distributed and extremely overdispersed with large outlying observations. Approximately 63% of the observations are zero-valued, with an overall mean of 38.47 and a standard deviation of 960.47. All of the zero-valued observations belong to inter-zonal flows off the main diagonal. The mean and standard deviation of inter-zonal flows are equal to 18.48 and 156.67, respectively. The maximum value is observed in the diagonal cell which corresponds to the intra-zonal flows occurring in Antwerp – the largest Flemish municipality – and is equal to 211681. In general, the majority of trips correspond to intra-zonal flows with the counts on the main diagonal accounting for approximately 51% of the total number of trips. The mean for intra-zonal flows is 6064.32, while the standard deviation is 15516.64.

The road network of Flanders with the corresponding borders of the 5 Flemish provinces, Antwerp, Limburg, East Flanders, Flemish Brabant and West Flanders, is presented in Figure 1. The circled areas indicate the capital-municipality of each province, the size of each circle is a relative representation of population size. Antwerp is the most populated capital, followed by Ghent, Leuven, Bruges and Hasselt. Brussels metropolitan area, which is also marked in the map, is not included in the analysis as it is a separate administrative center. In overall, the network runs a total length of 65296.72 kilometers and contains 97450 links which can be categorized into highways (8.58% including entrance/exit road segments), main regional roads (15.49%), small regional roads (21.1%), local municipal roads (52.91%) and walk/bicycle paths (1.92%).

3.2 Explanatory variables

The set of explanatory variables consists of six categorical variables and twelve discrete/continuous variables. The first five categorical variables capture the effects of intra-zonal flows measured in differences of 100 trips. Thus, these dummies take the value 100 if the trips are intra-zonal in municipalities (DM), cantons (DC), districts (DD) arrondissements (DA) provinces (DP) and 0 otherwise. These predictors capture individual effects; for instance, for intra-zonal flows in the main diagonal the municipality predictor DM will equal 100, whereas DC, DD, DA and DP will equal 0. The sixth categorical predictor (DE) is associated with the effect of higher education institutes in destination zones; it takes the value of 1 if the destination zone supports a college and/or a university and 0 otherwise. The set of covariates includes four discrete-valued variables which contain the total number of neighboring municipalities on canton (MC), district (MD), arrondissement (MA) and province (MP) levels for each corresponding OD pair. The rest of the covariates are continuous. Specifically, we include employment rate (ER), population density (PD; thousands inhabitants per square km), relative length of road networks (RL; road length in km's per surface area in square km's), perimeter length (PL) in km's, car ownership ratio (CR), yearly traffic in highways (HT) and in provincial/municipal roads (PMT) in km's, and finally distance (D) in km's. All covariates are used in logarithmic scale. Distance, of course, is zero for intra-zonal municipality flows and in order to use the logarithm it is set equal to 0.1, a value which for most practical purposes refers to negligible distance (100 meters). Furthermore, due to the particularity of the OD problem variables ER, PD, RL, PL, CR, HT and PMT come in pairs, i.e. each is used twice, one time for the origin-zone and one time for the destination-zone. The arguments for employing the continuous variables in pairs are the following; a) preliminary research revealed that it is better to use information for origin and destination zones separately rather than average, for instance, between origin and destination zones, b) having separate parameters estimates for origin and destination zones allows for elementary comparison with trip-production/attraction, c) using pairs on logarithmic scale and including distance provides an alternative interpretation of the Poisson mixture log-linear models as stochastic gravity, direct-demand models.

Most of the continuous variables were transformed to ratios relative to populations or surface areas. The specific transformations were chosen in order to maintain reasonable interpretations, but also in order to solve multicollinearity problems which were evidently present in raw variables. Analysis based on variance inflation factors (VIF) indicated no serious multicollinearity problems for the transformed variables with the highest VIF value being equal to 3.877.

4 Results

We start this section with a comparison between MCMC and INLA estimates for the PLN and PG models on an OD matrix of smaller scale. The full analysis for entire Flanders, including posterior and predictive inference based on MCMC, is presented next. Details

concerning M-H implementation are presented in Appendix A.

4.1 Comparing MCMC and INLA

The comparison presented here concerns a 10 by 10 OD matrix containing the flows between the 10 largest (in terms of population) Flemish municipalities. The rationale in choosing a smaller OD matrix is to evaluate how well can INLA approximate marginal posterior distributions under relatively small samples. The categorical predictors are not meaningful to use in this case, therefore, we use only employment rate, population density, length of road networks, highway traffic, provincial/municipal traffic and distance as covariates.

For fitting the reasons for considering a smaller OD are the following. First, INLA is based on the assumption of conditional independence for the Gaussian latent random field which means that the inverse covariance matrix is sparsely distributed allowing for fast and efficient Cholesky decomposition. In general, the assumption of conditional independence becomes stronger as the dimensionality of the random field increases. Therefore, we find it interesting to evaluate INLA on a smaller random field (i.e. 100 random effects, instead of 94864, plus the regression parameters). Second, INLA estimates the marginal posteriors either through Gaussian or through Laplace approximations based on Taylor's expansions around the posterior modes. Such approximations generally perform well when the sample size is large and the marginal posteriors are usually well centered around the posterior mode. Thus, we are interested in testing INLA on a smaller subset of the data.

For comparison purposes, we change the prior assumption for the intercept and the regression parameters. Specifically, instead of using the unit-information prior $\boldsymbol{\beta} \sim \mathbf{N}_{12}(\mathbf{0}, \boldsymbol{\Sigma}_{\boldsymbol{\beta}})$ with $\boldsymbol{\Sigma}_{\boldsymbol{\beta}} = n(\mathbf{X}^T\mathbf{X})^{-1}$, we assume independent normal priors with a large variance, namely $\boldsymbol{\beta} \sim \mathbf{N}_{12}(\mathbf{0}, \mathbf{I}_{12}\sigma^2)$ with $\sigma^2 = 10^3$. For fitting the PLN model through INLA, we used the R-INLA package (www.r-inla.org). We consider the 3 INLA approximating strategies, namely the Gaussian, the simplified Laplace and the Laplace approximations for marginal posterior distributions; see Rue et al. (2009) for details. In addition, as mentioned in Section 2.1, recent developments extend INLA to near-Gaussian latent models (Martins and Rue, 2013). The gamma prior is included in the available options of the R-INLA package, which gives us the opportunity to compare MCMC and INLA for the PG model as well.

Posterior means and standard deviations from M-H samples of 20000 draws and from the 3 INLA approximations for the PLN and PG models are presented in Table 1 and Table 2, respectively. The PLN intercept corresponds to that of the additive model formulation. As seen, the posterior PLN means from MCMC and INLA agree in general, especially under the simplified Laplace and Laplace approximations. The precision estimates slightly differ; the MCMC estimate is closer to the corresponding ML estimate which is 1.036. Also, the standard deviations from MCMC are overall lower. Concerning the PG model, the INLA Laplace seems to provide more accurate estimates which are closer to the MCMC estimates in comparison to the Gaussian and simplified Laplace approaches. Standard deviations are more or less the same for this model. Marginal posterior distribution

PLN estimates				
Parameter	**M-H**	**INLA**		
		Gaussian	**Simplified Laplace**	**Laplace**
β_0 intercept	-1.031 (2.288)	-1.022 (2.623)	-1.061 (2.623)	-1.061 (2.623)
β_1 ER (o)	0.763 (0.865)	0.749 (0.985)	0.755 (0.985)	0.755 (0.985)
β_2 ER (d)	1.826 (0.883)	1.802 (0.979)	1.824 (0.979)	1.824 (0.979)
β_3 PD (o)	0.406 (0.420)	0.391 (0.476)	0.401 (0.476)	0.401 (0.476)
β_4 PD (d)	1.414 (0.425)	1.401 (0.477)	1.420 (0.477)	1.420 (0.477)
β_5 RL (o)	0.697 (0.779)	0.684 (0.892)	0.689 (0.891)	0.689 (0.891)
β_6 RL (d)	-0.060 (0.805)	-0.048 (0.895)	-0.057 (0.894)	-0.057 (0.894)
β_7 HT (o)	-0.297 (0.154)	-0.291 (0.180)	-0.291 (0.180)	-0.291 (0.178)
β_8 HT (d)	0.194 (0.156)	0.181 (0.180)	0.187 (0.180)	0.187 (0.180)
β_9 PMT (o)	0.891 (0.225)	0.897 (0.260)	0.901 (0.260)	0.901 (0.260)
β_{10}PMT (d)	0.886 (0.220)	0.889 (0.260)	0.890 (0.260)	0.890 (0.259)
β_{11}D	-1.129 (0.048)	-1.131 (0.057)	-1.135 (0.057)	-1.135 (0.057)
$\tau(1/\sigma^2)$	0.989 (0.139)	0.906 (0.139)	0.906 (0.139)	0.906 (0.139)

Table 1: Posterior means and standard deviations (in parentheses) from a M-H sample of 20000 draws and from the 3 INLA approaches for the PLN model; (o) refers to origin effects, (d) to destination effects.

PG estimates				
Parameter	**M-H**	**INLA**		
		Gaussian	**Simplified Laplace**	**Laplace**
β_0 intercept	-2.013 (2.488)	-2.147 (2.496)	-2.087 (2.496)	-2.052 (2.484)
β_1 ER (o)	1.081 (0.925)	1.039 (0.918)	1.016 (0.918)	1.058 (0.913)
β_2 ER (d)	1.542 (0.895)	1.486 (0.901)	1.473 0.901)	1.515 (0.897)
β_3 PD (o)	0.507 (0.428)	0.512 (0.441)	0.526 (0.441)	0.513 (0.439)
β_4 PD (d)	1.282 (0.440)	1.271 (0.434)	1.289 (0.434)	1.272 (0.432)
β_5 RL (o)	0.765 (0.785)	0.718 (0.781)	0.757 (0.781)	0.763 (0.776)
β_6 RL (d)	0.078 (0.823)	-0.033 (0.810)	0.012 (0.810)	0.022 (0.805)
β_7 HT (o)	-0.431 (0.180)	-0.434 (0.177)	-0.436 (0.177)	-0.440 (0.176)
β_8 HT (d)	0.056 (0.188)	0.077 (0.171)	0.073 (0.171)	0.068 (0.170)
β_9 PMT (o)	1.082 (0.246)	1.099 (0.243)	1.087 (0.243)	1.095 (0.242)
β_{10}PMT (d)	1.163 (0.232)	1.166 (0.232)	1.156 (0.232)	1.161 (0.231)
β_{11}D	-1.184 (0.079)	-1.168 (0.081)	-1.168 (0.081)	-1.181 (0.082)
θ	1.070 (0.123)	1.070 (0.142)	1.070 (0.142)	1.070 (0.142)

Table 2: Posterior means and standard deviations (in parentheses) from a M-H sample of 20000 draws and from the 3 INLA approaches for the PG model; (o) refers to origin effects, (d) to destination effects.
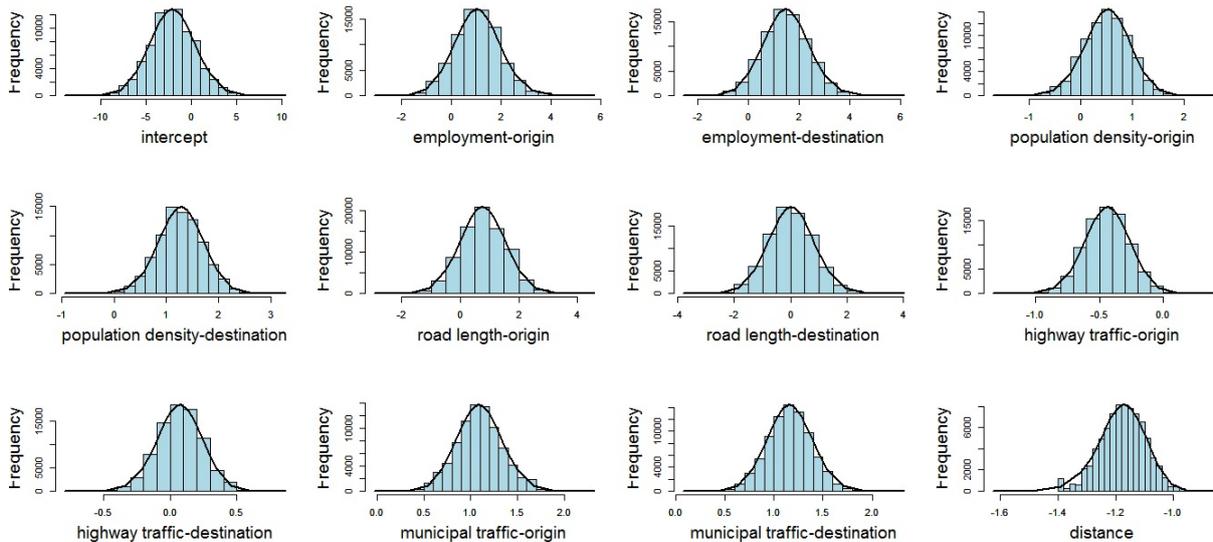
Figure 2: Histograms of PG regression parameters from 20000 posterior draws and estimates of the posterior marginals (black lines) from INLA based on the Laplace approximation

estimates for the regressors of the PG model under the Laplace approximation are shown in Figure 2; as seen the estimates approximate particularly well the histograms derived from MCMC. The corresponding figures for the PLN model (not presented here) are equivalent.

In conclusion, we find that INLA provides a fast and efficient alternative to MCMC under specific prior assumptions, which makes it a potentially promising tool for OD modeling on large scale networks. It is worth mentioning that INLA runtimes were 2.64 sec's for the PG model and 2.14 sec's for the PLN model. On the other hand, 21000 M-H iterations (we used the first 1000 as burn-in) required 14.82 sec's for the PG model and approximately 21 min's for the PLN model due to additional numerical integration within MCMC. Thus, INLA is particularly useful for the PLN model. Arguably, in medium-sized examples like this one, using MCMC for the hierarchical data-augmented PLN model could be more efficient than MCMC with numerical integration for the marginal likelihood. We tested this using WinBUGS (Spiegelhalter et al., 2003), nevertheless, the sampler failed to converge even after 200000 iterations. All computations were performed in a standard 64-bit laptop with 2.20 GHz CPU and 4 GB of RAM using R version 3.0.1. The R code used for INLA and the subset of the OD data are provided as supporting material.

Despite these advantages, we find that the R-INLA package is still restrictive with respect to certain aspects and requires further development which will allow for more general modeling frameworks. In particular, the package does not yet fully support mul-

tivariate prior assumptions such as g-prior structures (e.g. Zellner, 1986) for regression coefficients. Moreover, it would be interesting to include further distributional options covering near-Gaussian latent fields, such as the inverse-Gaussian prior considered in this paper.

4.2 Posterior inference for Flanders

Posterior means and 95% credible intervals based on 4000 posterior draws are presented in Table 3. The corresponding INLA Gaussian estimates for the PG and PLN models are presented in Appendix B. The INLA estimates are slightly different due to the different prior assumption, namely $\boldsymbol{\beta} \sim \mathbf{N}_{12}(\mathbf{0}, \mathbf{I}_{12}\sigma^2)$ with $\sigma^2 = 10^3$. Nevertheless, the overall conclusions discussed next are also supported by the INLA estimates. Details of M-H implementation and a comparison of MCMC and INLA runtimes can be found in Appendix A. In general, the posterior means of the PLN and PIG models are more similar. For instance, parameters β_0, β_6, β_9, β_{10}, β_{14} and β_{18} of the PG model are substantially different from the corresponding estimates of the other two models, especially the intercept estimate. On the other hand, parameters β_{11}, β_{12} and β_{20} differ across models.

The parameters β_1 to β_5 of the categorical variables are all positive except of the last parameter for intra-zonal municipality trips. The positive effects of β_1 to β_4 are to be expected, since the OD flows are generally larger in diagonal blocks of cells of the OD matrix corresponding to intra-zonal flows for the various administrative levels. The negative sign of β_5 is not expected but it might be explained as simply counterbalancing the absence of the strong negative effect of distance which is set almost equal to zero for intra-zonal municipality trips. Parameter β_6 is positive which leads to the consistent interpretation that destination zones which support a college or a university are more likely to attract trips than zones without a college/university.

Parameters β_7 to β_{10} quantify the influence of the total number of surrounding municipalities on the levels of cantons, districts, arrondissements and provinces, respectively. This effect is in general not straightforward to predict, nevertheless the parameter estimates provide some insights. On the small-scale level of cantons parameter β_7 has a positive sign, whereas on the large-scale levels of districts, arrondissements and provinces – where the total number of municipalities increase and a spead-out of trips is more likely – the corresponding parameters β_8, β_9 and β_{10} are negative. This implies that the effect changes from positive to negative when exceeding a specific radius threshold of distance. Recent transportation studies discuss similar ideas such as the *neighborhood-effect* concept investigated in more detail by Sohn and Kim (2010).

Regarding the continuous variables used in pairs, the more general explanatory variables have parameters with positive signs, namely population density (β_{13},β_{14}), perimeter length (β_{17},β_{18}) and kilometers-driven in highways (β_{21},β_{22}) and provincial/municipal roads (β_{23},β_{24}). The uniformly positive effects for origin and destination zones do not come as a surprise, since we would expect these four variables to be positively correlated with trip-production (origin zones) as well as trip-attraction (destination zones). In contrast, the parameters of employment rate (β_{11},β_{12}), relative length of road network

(β_{15},β_{16}) and car ownership ratio (β_{19},β_{20}) have opposite signs for origin and destination effects.

In transportation studies employment rate is commonly associated with trip-attraction models (see e.g. Yao and Morikawa, 2005). In accordance, the posterior estimate of employment rate is positive for destination zones and negative for origin zones which leads to the rational interpretation that zones with high employment rates are more likely to attract trips rather than to generate trips. The relative length of road networks is associated with the concept of *accessibility* (see e.g. Odoki et al., 2001), a concept which is present primarily in trip-attraction studies. In general, a larger relative length in the network, will decrease the friction of travel (e.g. distance, time) significantly, and thus increase accessibility. The posterior mean is positive for destination zones and negative for origin zones. Consistently, this implies that zones with high levels of accessibility are more likely to attract trips than low-accessible zones. Conversely, high-accessible zones are less likely to produce trips than low-accessible zones. A possible explanation for the negative origin effect is that high levels of accessibility within a zone might encourage intra-zonal trips and reduce outgoing trips. Car ownership is traditionally used as an explanatory variable with positive impact in trip-production models. In agreement, the posterior mean for car ownership is positive for origin zones, which means that zones with high car ownership ratios also have high trip-production rates. The estimate is negative for destination zones implying that high car ownership ratios are negatively correlated with trip-attraction. The negative destination effect may be attributed to congestion issues.

Distance with parameter β_{25} is the final variable. Distance is a key variable in gravity-type and direct-demand models, since it is directly related to the costs of the deterrence function used within the trip-distribution step. In our model distance has a negative posterior mean which accords with the basic deterrent gravitational assumption of trip-distribution models. Furthermore, based on the posterior mean over standard deviation ratio, distance is the most significant explanatory variable in all models.

Table 3 also includes the values of the AIC, BIC and marginal/hierarchical DIC. The posterior mean of the deviance is used for the calculation of AIC and BIC. The three criteria provide more support to the PLN and PIG models, which provides a justification for the similarity of the posterior estimates from the two models. Furthermore, all three criteria indicate that the PIG distribution is the most appropriate marginal sampling distribution. The hierarchical DIC is calculated based on reduced samples of 500 draws, due to memory limitations given the large dimensionality of the data-augmented space. In addition, sampling the random effects of the PLN model is relatively complicated and time-consuming, therefore we focus on the PG and PIG models for the remainder of this paper. Based on the hierarchical DIC it is difficult to distinguish which hierarchical model is more appropriate for predictive purposes, since the differences between the PG and PIG are marginal.

The random effects present some dissimilarities between the two models. The range of the PG random effects is from 3.81×10^{-8} to 40.61 (-17.83 to 3.71 on log-scale), while the PIG random effects range from 9.48×10^{-3} to 132.35 (-4.66 to 4.89 on log-scale).

Parameter	PG		PLN		PIG	
	Mean	95% Cr. Int.	Mean	95% Cr. Int.	Mean	95% Cr. Int.
β_0	4.027	(3.214, 4.869)	6.104	(5.230, 6.989)	6.847	(6.028, 7.675)
β_1 DP	0.005	(0.005, 0.005)	0.005	(0.005, 0.006)	0.006	(0.005, 0.006)
β_2 DA	0.007	(0.007, 0.008)	0.007	(0.007, 0.008)	0.008	(0.007, 0.008)
β_3 DD	0.008	(0.008, 0.009)	0.008	(0.008, 0.009)	0.009	(0.008, 0.009)
β_4 DC	0.008	(0.007, 0.009)	0.006	(0.006, 0.007)	0.006	(0.006, 0.007)
β_5 DM	-0.082	(-0.083, -0.080)	-0.086	(-0.087, -0.084)	-0.084	(-0.086, -0.083)
β_6 DE	0.424	(0.388, 0.460)	0.535	(0.496, 0.574)	0.536	(0.497, 0.581)
β_7 MC	0.473	(0.435, 0.510)	0.461	(0.422, 0.501)	0.450	(0.411, 0.490)
β_8 MD	-0.494	(-0.542, -0.445)	-0.441	(-0.491, -0.391)	-0.442	(-0.489, -0.392)
β_9 MA	-0.088	(-0.124, -0.055)	-0.188	(-0.225, -0.149)	-0.210	(-0.249, -0.167)
β_{10} MP	-0.491	(-0.636, -0.345)	-0.737	(-0.888, -0.589)	-0.783	(-0.924, -0.636)
β_{11} ER(o)	-1.062	(-1.207, -0.918)	-0.482	(-0.629, -0.334)	-0.240	(-0.383, -0.105)
β_{12} ER(d)	0.326	(0.194, 0.462)	0.492	(0.345, 0.641)	0.608	(0.460, 0.759)
β_{13} PD(o)	0.505	(0.477, 0.533)	0.499	(0.470, 0.528)	0.500	(0.474, 0.529)
β_{14} PD(d)	0.577	(0.548, 0.606)	0.626	(0.594, 0.658)	0.631	(0.595, 0.662)
β_{15} RL(o)	-0.315	(-0.359, -0.272)	-0.318	(-0.365, -0.272)	-0.334	(-0.380, -0.289)
β_{16} RL(d)	0.280	(0.236, 0.322)	0.267	(0.220, 0.315)	0.265	(0.219, 0.310)
β_{17} PL(o)	1.253	(1.208, 1.298)	1.289	(1.241, 1.338)	1.283	(1.238, 1.327)
β_{18} PL(d)	0.430	(0.385, 0.475)	0.500	(0.452, 0.549)	0.509	(0.459, 0.559)
β_{19} CR(o)	3.454	(3.149, 3.762)	3.413	(3.095, 3.731)	3.520	(3.227, 3.831)
β_{20} CR(d)	-1.465	(-1.768, -1.180)	-1.255	(-1.577, -0.939)	-1.081	(-1.386, -0.752)
β_{21} HT(o)	0.010	(0.007, 0.014)	0.011	(0.008, 0.015)	0.010	(0.007, 0.014)
β_{22} HT(d)	0.052	(0.049, 0.056)	0.050	(0.047, 0.054)	0.050	(0.046, 0.053)
β_{23} PMT(o)	0.270	(0.250, 0.289)	0.278	(0.257, 0.299)	0.275	(0.254, 0.294)
β_{24} PMT(d)	0.869	(0.850, 0.888)	0.876	(0.853, 0.898)	0.870	(0.849, 0.891)
β_{25} D	-2.906	(-2.927 -2.885)	-2.984	(-3.007, -2.960)	-2.936	(-2.957, -2.915)
θ	0.965	(0.947, 0.983)	-			-
σ^2		-	1.065	(1.043, 1.086)		-
ζ		-		-	0.377	(0.359, 0.399)
AIC		281519.3		279364.7		278468.9
BIC		281774.7		279620.1		278724.3
DIC (marginal)		281492.4		279337.7		278441.4
DIC (hierachical)		224141.4		-		224146.1

Table 3: Posterior means and 95% credible intervals for regression and dispersion parameters and the values of AIC, BIC, marginal DIC and hierarchical DIC.
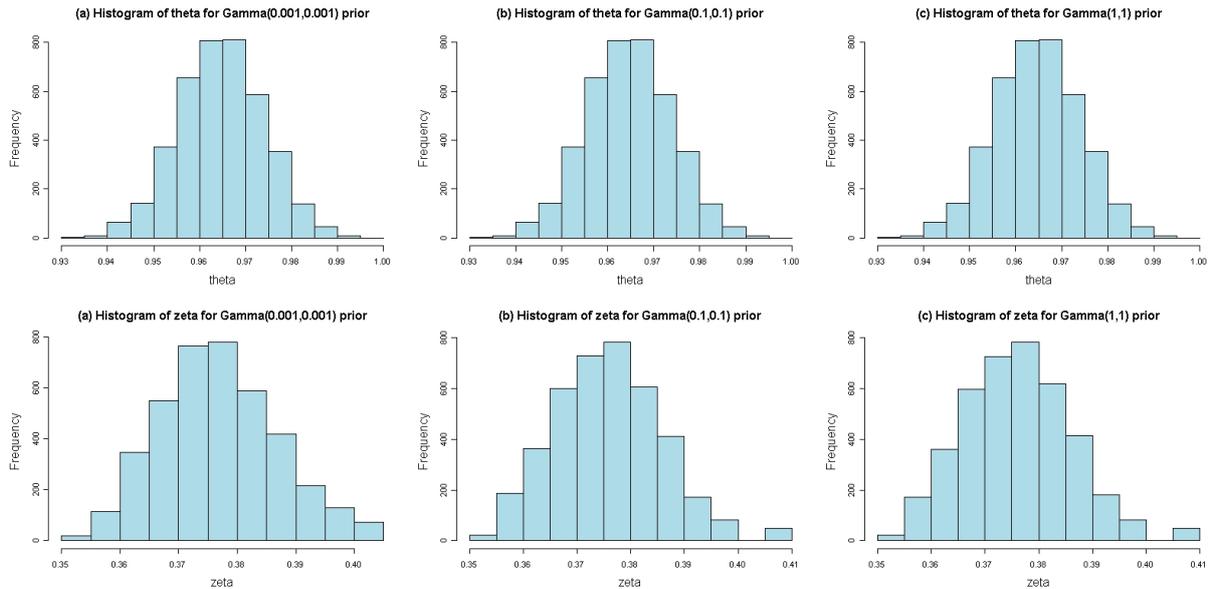
Figure 3: Histograms of dispersion parameters θ (top) and ζ (bottom) under gamma hyperpriors with a equal to; (a) 0.001, (b) 0.1 and (c) 1.

Due to the GIG posterior distribution, the PIG random effects exhibit a longer right-tail than the PG random effects which are gamma distributed. On logarithmic scale the PIG random effects are relatively more symmetrical near 0, whereas the PG random effects have a longer left-tail.

4.3 Sensitivity analysis for hyperpriors

In this section we perform a sensitivity analysis for parameter a of the gamma hyperpriors assigned to parameters θ and ζ of the PG and PIG models. Parameter σ^2 is not included in the analysis, due to the substantial time which is required for M-H simulation from the PLN model. Histograms of 4000 posterior draws of parameters θ and ζ for values of a equal to 0.001 (the initial value), 0.1 and 1 are presented in Figure 3. As seen, the posterior distributions are not influenced by hyperparameter a. One can notice a slight change in the right tail of the posterior distribution of ζ for a equal to 0.1 and 1, nonetheless this does not affect posterior inferences. The results are in line with the discussion in Gelman (2006), since in our case the random effects are observational and therefore we would not expect to have the sensitivity problems that arise in grouped random effects settings for small numbers of groups.

17

4.4 Posterior predictive checks for OD flows

For overall goodness-of-fit, we employ posterior predictive checks (Meng, 1994) for the absolute and squared distances (with respect to the expected values) and for the hierarchical deviance. The absolute distance is more sensitive to small deviations, whereas squared distance assigns more penalty to large deviations. Each test quantity is calculated for observed and predicted data over the 500 posterior draws.

Test quantity	Formula	PG	PIG
Absolute distance	$\sum \left(\mathbf{y} - E(\mathbf{y}|\boldsymbol{\beta}, \mathbf{u}) \right)$	0.278	0.440
Squared distance	$\sum \left(\mathbf{y} - E(\mathbf{y}|\boldsymbol{\beta}, \mathbf{u}) \right)^2$	0.532	0.488
Deviance	$-2 \log p(\mathbf{y}|\boldsymbol{\beta}, \mathbf{u})$	0.996	0.648

Table 4: Bayesian p-values for the absolute distance, squared distance and deviance test quantities from 500 posterior draws of the hierarchical PG and PIG models.

The test quantities with the corresponding Bayesian p-values are presented in Table 4. In general, both models provide satisfactory Bayesian p-values for squared distances, which are close to the ideal value of 0.5. Predictions from the PIG seem to replicate better the observed data for small deviations from the expected values and also with respect to the Poisson distributional assumption. Note that the aim here is not model comparison, but examination of the characteristics of predictions.

An interesting feature of OD modeling is that the administrative structure allows for various aggregations of observed and replicated data with respect to administrative levels and also types of trips. From a statistical perspective, the aggregated distributions can be compared to the observed aggregated values, thus resulting in Bayesian p-values for case-specific tests. Examples of such tests for incoming trips to the municipality of Antwerp, total trips for Flanders and intra-zonal trips for the five Flemish provinces are presented in Figure 4. In general, all p-values are within acceptable limits. From a transportation planning perspective, such predictions are particularly useful for policy-evaluation.

4.5 Predictive inference for link flows

For traffic-assignment we utilize the deterministic user equilibrium (DUE) model which is based on Wardrop's 1st principle (Wardrop, 1952), also known as the *equilibrium principle*. In short, DUE assignment uses an iterative process in order to reach a convergent solution in which travelers cannot reduce their travel times by switching routes. At each iteration link capacity restraints and link flow-dependent travel times are taken into account in order to calculate link flows. As *link performance function* we adopt the common BPR formulation (Bureau of Public Roads, 1964) which relates link travel times to volume-over-capacity (V/C) ratios, specifically $t = t_f[1 + \alpha(v/c)^\beta]$, where t is the link travel time, t_f is link free-flow travel time, v is link volume (flow), c is link capacity and α, β are calibration parameters which are set equal to their historical values of 0.15 and 4,
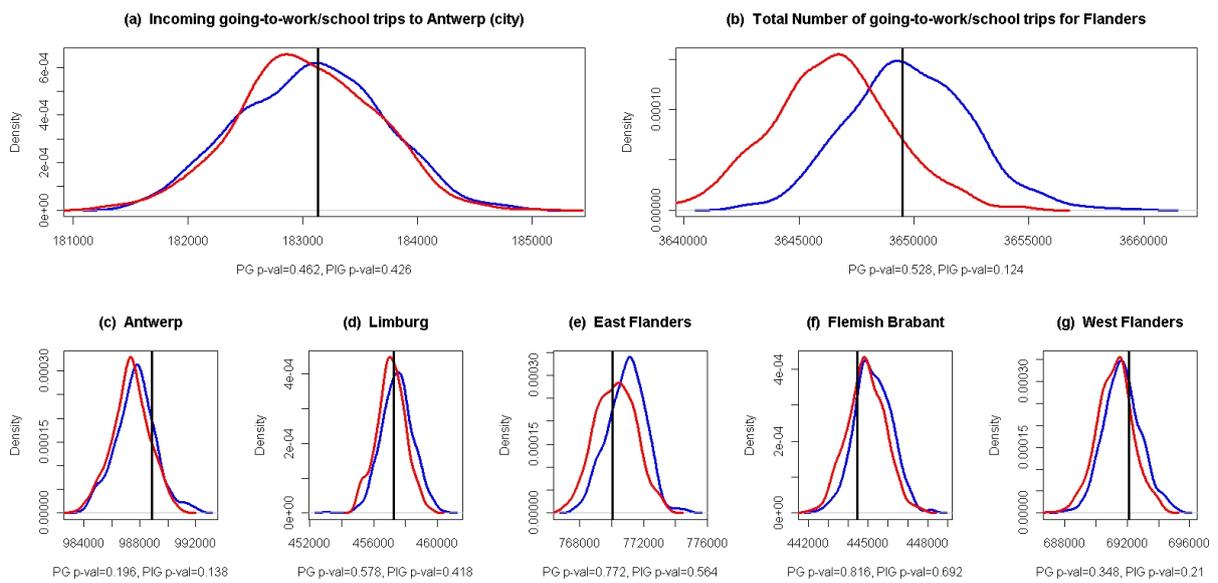
Figure 4: Kernel estimates of predictive distributions for going-to-work/school trips from the PG model (in blue) and the PIG model (in red) for (a) incoming trips to the city of Antwerp, (b) total number of trips in Flanders and intra-zonal trips for the five Flemish provinces; (c) Antwerp, (d) Limburg, (e) East Flanders, (f) Flemish Brabant and (g) West Flanders. The vertical black lines indicate the observed quantities.
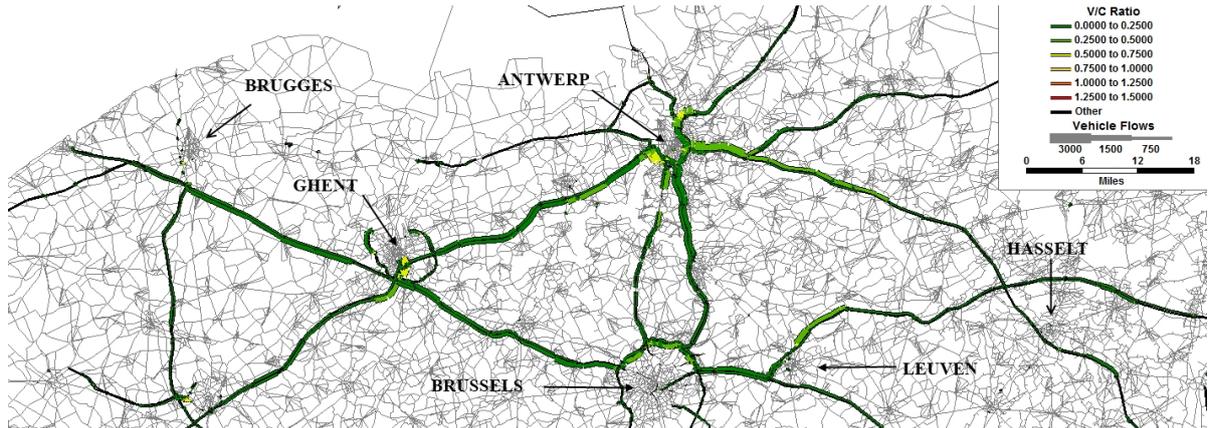
Figure 5: Mean visualization of highway flows and V/C ratios for going-to-work/school trips between 7-8 am in Flanders under DUE assignment and PIG OD predictions.

respectively. If we denote by $\mathbf{A}$ the DUE assignment operator, we execute 500 individual assignments from the predictive OD's of each model and obtain 500 corresponding link flow or link volume vectors $\mathbf{v}$. That is, $\mathbf{A}\mathbf{y}^{pred(m)} = \mathbf{v}^{(m)}$ for $m = 1, 2, ..., 500$, where $\mathbf{v}^{(m)} = (v_1^{(m)}, v_2^{(m)}, ..., v_l^{(m)})^T$ and l is the total number of network links. For the Flemish network l is equal to 97450. The assignments concern the morning peak-hour interval between 7 am and 8 am for a normal weekday.

The mean state of the Flemish network under DUE assignment and OD predictions from the PIG model is presented in Figure 5. By "mean state" it is meant that the 500 link flow vectors were averaged first and the visualized. In order to make Figure 5 simpler to comprehend only volumes and V/C ratios for highway links are highlighted. The main findings are the following. V/C ratios are higher in specific segments on or near the highways rings of Antwerp (R1) and Ghent (R4), which can be identified by the yellow spots indicating V/C ratios between 0.5 and 0.75. Relatively high V/C ratios (light green colour) also occur on the northern part of highway ring R0 around Brussels, on highway E40 near Leuven, highway E313 which connects Antwerp with Hasselt and to a lesser degree on highways E17 and E19 which connect Antwerp with Ghent and Brussels, respectively. The corresponding visualization map based on PG predictions is not presented as it seems almost identical to the one in Figure 5, with differences being difficult to spot on a global scale.

An interesting application is the identification of congested links on the network. Congestion identification is related to *critical link* identification, which is customarily a subject of *vulnerability analysis* and relies significantly on traffic-assignment procedures (see e.g. Jenelius et al., 2006). Through our approach congested links are evaluated directly in terms of probability estimates. As congested links we define those links on which the V/C ratio exceeds a certain threshold value t with a certain probability $P(\text{V/C} > t)$. As a conservative choice and in order not to overestimate the number of critical links a threshold value of 0.95 is adopted, based on the assumption that the majority of trips
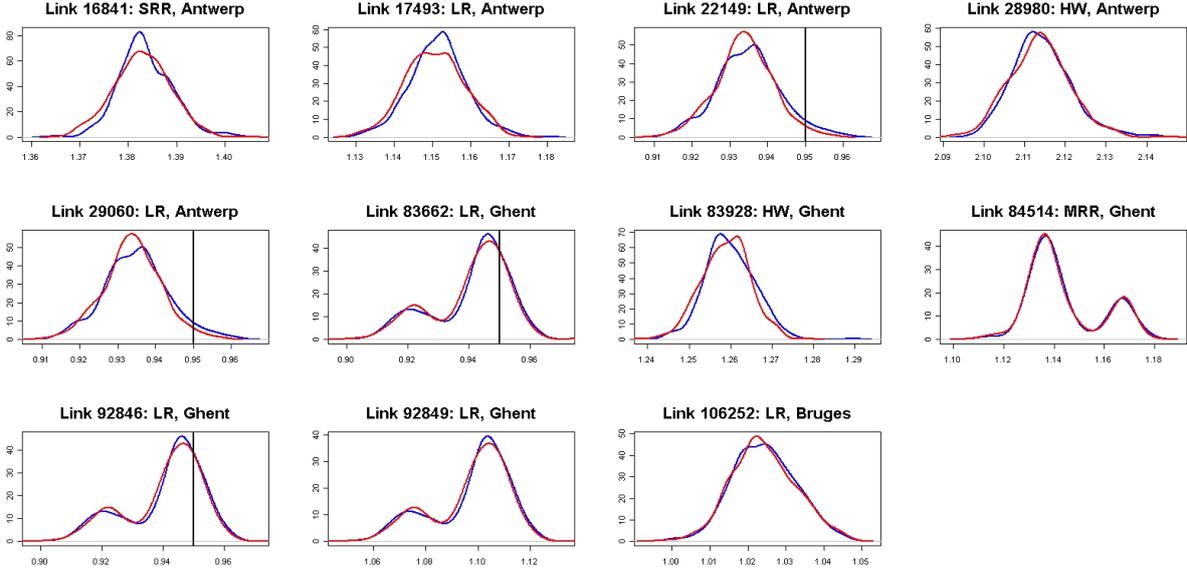
20

Figure 6: Kernel estimates of the PG (in blue) and PIG (in red) V/C distributions of the 11 congested links which either include or exceed the threshold value of 0.95 highlighted by a vertical black line in the distributions which include this value. The abbreviations HW, MRR, SRR and LR stand for highways, main regional roads, small regional roads and local roads.

taking place between 7 am and 8 am are either work or school related trips. For $t = 0.95$ congestion is identified in eleven links which all belong to large Flemish municipalities; 5 in Antwerp, 5 in Ghent and 1 link in Bruges. The V/C distributions from both models are presented in Figure 6.

Certain remarks can be made, based on Figure 6, regarding V/C distributions and consequently link flow distributions from DUE assignment. First, the choice of statistical model does not seem to affect individual V/C distributions as the corresponding distributions are very similar. Second, individual V/C and link distributions are not necessarily close to normal distributions – for instance bimodalities are observed – in contrast to aggregated distributions (e.g. link flows for highways – not presented here) which converge to normality in accordance to the central limit theorem. Third, the bimodalities may be attributed to the iterative user equilibrium procedure; when the flows on a specific link and at a given iteration exceed a certain threshold – leading to a high V/C ratio – and there exists an alternative link which has a cost which is close but lower, then in the following iteration a switch of flows will occur from the high-cost link to the low-cost link. This "switching" effect will eventually result to bimodal distributions as the ones observed in Figure 6.

Seven out of the eleven links have a V/C value greater than 0.95 with probability 1. Visual examination of the distributions in Figure 6 additionally reveals that these

Congested link	Link type	PG		PIG	
		$E(V/C)$	$P(V/C > 0.95)$	$E(V/C)$	$P(V/C > 0.95)$
16841	Small regional road	1.384	1	1.383	1
17493	Local road	1.152	1	1.151	1
22149	Local road	0.935	0.046	0.934	0.022
28980	Highway	2.114	1	2.114	1
29060	Local road	0.935	0.046	0.934	0.022
83662	Local road	0.941	0.236	0.941	0.208
83928	Highway	1.260	1	1.259	1
84514	Main regional road	1.144	1	1.144	1
92846	Local road	0.941	0.236	0.941	0.208
92849	Local road	1.098	1	1.097	1
106252	Local road	1.024	1	1.024	1

Table 5: Expected V/C ratios and probabilities of exceeding a V/C of 0.95 for the 11 congested links under DUE assignment and PG, PIG predictions.

seven links also exceed the value $t = 1$ with probability 1, except perhaps of link 106252 which has its minimum located near 1 and may therefore include smaller values than 1 with a low probability. The remaining four links have lower V/C ratios and exceed the value 0.95 with a probability lower than one. The expected values and the corresponding probabilities for the eleven congested links are presented in Table 5. Assignment with PG predictions results to slightly higher probabilities for links 22149, 29060, 83662 and 92846. We also note that if the analysis was based on the expected values congestion would not have been identified on those four links.

5   Discussion

In this paper we investigated the use of Poisson mixtures in OD modeling as a viable alternative to traditional transportation models. The advantages of the proposed approach are; i) it incorporates the steps of trip-generation and trip-distribution in statistical models which provide a wider inferential scope and ii) it allows for probabilistic inference on link traffic and congestion, conditional on the assignment model. At the same time, the approach may be viewed as a statistical, direct-demand, gravity model, thus retaining a strong relation with traditional transportation models.

The case study focused on a large, sparsely distributed and overdispersed OD matrix derived from the 2001 Belgian travel census covering the region of Flanders. In particular, we considered the PG, PLN and PIG models as alternative modeling options. The PIG – a model not as popular as its competing alternatives – provided the best marginal fit and resulted in consistent short-term predictions. Given the convenient distributional properties of the PIG model, we recommend its use when analyzing large-scale OD matrices.

In addition, we investigated the performance of INLA compared to MCMC for the PG and PLN models and found that INLA can provide fast and accurate approximations. From this point of view, INLA is particularly suited for the PLN, which proved to be the most cumbersome model to work with using MCMC. Further development of the R-INLA package, in terms of prior extensions, will make it a useful tool for large-scale OD analysis.

Future research directions concerning transportation issues are many. First, the set of covariates used in this study is by no means conclusive. As pointed out by one referee the models could improve in terms of capturing representation of activities in destination-zones. This can be achieved by including number of workplaces and shopping facilities as predictors. This type of information was not available and could not be included in the current analysis. Second, the issue of modal-split which was not pursued here can be potentially incorporated in the proposed modeling approach. A third issue concerns dynamic modeling of short-term OD matrices, for example analysis of OD matrices on hourly intervals. A fourth category of issues is related to a series of traffic-assignment comparative studies between the DUE model, utilized here, and other assignment models such as the stochastic user equilibrium model, conditional on Bayesian predictions.

From a statistical perspective, discrete random effects could have been considered as an alternative approach for clustering purposes. This approach was not pursued here as the focus of this study was on modeling and capturing the heterogeneity per OD pair. Finally, the PIG model can be of potential value to any other count data analysis problem under the presence of overdispersion. From this point of view, it will be interesting to consider zero-inflated model extensions and also to compare to other mixing/prior distributional designs.

Acknowledgements

Appendix A: Metropolis-Hastings simulation

We utilize M-H simulation on the marginal structures in order to bypass sampling 94864 random effects at each MCMC iteration. Although sampling $\mathbf{u}$ in a Gibbs-like fashion is straightforward for the hierarchical PG and PIG models, memory limitations would require discarding $\mathbf{u}$ at the end of each iteration. M-H for the marginal PG and PIG structures is far more efficient with $\boldsymbol{\beta}$, θ and ζ being easy to sample, while $\mathbf{u}$ can be generated subsequently as described in sections 2.1 and 2.3. The PLN model is more problematic since an additional Metropolis step or rejection sampling is required for the hierarchical structure, which is an obvious burden for 94864 random effects. On the other hand, simulation for the marginal PLN structure requires numerical or MC integration within MCMC and – in addition – vector $\mathbf{u}$ is not easy to sample subsequently.

In particular, we employ an independence-chain M-H algorithm where the location and scale of the proposals are fixed (see e.g. Chib and Greenberg, 1995) to the corresponding ML estimates. For regression vector $\boldsymbol{\beta}$ a multivariate normal proposal is used, i.e. $q(\boldsymbol{\beta}) = \mathbf{N}_{p+1}(\boldsymbol{\beta}^{ML}, \mathbf{V}_{\boldsymbol{\beta}}^{ML})$ with $\boldsymbol{\beta}^{ML}$ being the ML estimate of $\boldsymbol{\beta}$ and $\mathbf{V}_{\boldsymbol{\beta}}^{ML}$ the estimated variance-covariance matrix of $\boldsymbol{\beta}^{ML}$ for each model. For the dispersion parameters θ, σ^2 and ζ we used the following gamma proposals; $q(\theta) = Gamma(a_{PG}, b_{PG})$, $q(\sigma^2) = Gamma(a_{PLN}, b_{PLN})$ and $q(\zeta) = Gamma(a_{PIG}, b_{PIG})$ with proposal parameters set to satisfy the conditions $a_{PG}/b_{PG} = \theta^{ML}$, $a_{PG}/b_{PG}^2 = Var(\theta^{ML})$, $a_{PLN}/b_{PLN} = \sigma^{2ML}$, $a_{PLN}/b_{PLN}^2 = Var(\sigma^{2ML})$, $a_{PIG}/b_{PIG} = \zeta^{ML}$ and $a_{PIG}/b_{PIG}^2 = Var(\zeta^{ML})$. Regarding probability calculations from the PLN distribution we implemented both numerical and MC integration. Results showed that the MC sample L should be preferably 2000 in order to obtain stable estimates, similar to the estimates from numerical integration, while numerical integration was already two-times faster than MC integration with a sample of 200. Therefore, numerical integration was preferred.

We utilized 5 independent M-H chains of size 4200 and discarded the first 200 iterations as burn-in, resulting in posterior samples of 20000 draws. The 10th, 30th, 50th, 70th and 90th percentile points of the proposal distributions were used starting values. The resulting acceptance ratios were 72% for the PG model, 67% for the PLN model and 33% for the PIG model, on average. The multi-chain diagnostics of Gelman and Rubin (1992) and Brooks and Gelman (1998) were used to asses convergence. All univariate potential scale reduction factors (PSRF) were very close to 1 for all 3 models. The multivariate PSRF for the PG, PLN and PIG were 1.01, 1.01 and 1.06, respectively. Finally, in order to reduce the computational burden of the subsequent analysis the posterior samples were thinned by an interval of 5, resulting in final posterior samples of 4000 draws.

Implementation of MCMC was done in R version 2.8.2 on a 64bit Windows Server 2003 R2 with 32 GB of RAM. The simulations for the PG and PIG models required approximately 1 and 2.4 hours, respectively, whereas the PLN model required 3.6 days due to numerical integration.

The INLA models based on the prior assumption $\boldsymbol{\beta} \sim \mathbf{N}_{26}(\mathbf{0}, \mathbf{I}_{26}\sigma^2)$, with $\sigma^2 = 10^3$,

were fitted remotely in R version 3.0.1 through the Linux Server maintained by the INLA support team. The PG model required approximately 2.2 hours and the PLN model about 2.5 hours. The Gaussian approximation was used for both models.

Appendix B: INLA estimates

Here we present the INLA estimates for the PG and PLN models using the Gaussian approximation for the entire dataset.

Parameter	PG		PLN	
	Mean	95% Cr. Int.	Mean	95% Cr. Int.
β_0	3.605	(2.903, 4.307)	5.974	(5.106, 6.847)
β_1 DP	0.005	(0.005, 0.005)	0.005	(0.005, 0.005)
β_2 DA	0.007	(0.006, 0.007)	0.007	(0.006, 0.007)
β_3 DD	0.008	(0.007, 0.008)	0.008	(0.008, 0.009)
β_4 DC	0.008	(0.007, 0.008)	0.007	(0.006, 0.008)
β_5 DM	-0.082	(-0.084, -0.081)	-0.078	(-0.080, -0.076)
β_6 DE	0.435	(0.404, 0.466)	0.509	(0.471, 0.547)
β_7 MC	0.459	(0.427, 0.491)	0.431	(0.392, 0.470)
β_8 MD	-0.482	(-0.523, -0.442)	-0.424	(-0.472, -0.376)
β_9 MA	-0.079	(-0.109, -0.048)	-0.177	(-0.214, -0.139)
β_{10} MP	-0.447	(-0.569, -0.324)	-0.699	(-0.848, -0.551)
β_{11} ER(o)	-1.037	(-1.163, -0.911)	-0.458	(-0.603, -0.313)
β_{12} ER(d)	0.310	(0.192, 0.428)	0.449	(0.302, 0.596)
β_{13} PD(o)	0.495	(0.471, 0.519)	0.469	(0.440, 0.498)
β_{14} PD(d)	0.558	(0.533, 0.583)	0.591	(0.560, 0.622)
β_{15} RL(o)	-0.315	(-0.353, -0.278)	-0.299	(-0.344, -0.254)
β_{16} RL(d)	0.287	(0.250, 0.324)	0.253	(0.208, 0.298)
β_{17} PL(o)	1.272	(1.232, 1.312)	1.212	(1.165, 1.259)
β_{18} PL(d)	0.442	(0.402, 0.482)	0.479	(0.429, 0.528)
β_{19} CR(o)	3.401	(3.140, 3.663)	3.183	(2.871, 3.495)
β_{20} CR(d)	-1.549	(-1.813, -1.286)	-1.177	(-1.496, -0.859)
β_{21} HT(o)	0.010	(0.007, 0.012)	0.010	(0.007, 0.014)
β_{22} HT(d)	0.051	(0.048, 0.054)	0.047	(0.043, 0.050)
β_{23} PMT(o)	0.264	(0.246, 0.281)	0.263	(0.242, 0.283)
β_{24} PMT(d)	0.867	(0.850, 0.884)	0.824	(0.802, 0.846)
β_{25} D	-2.912	(-2.930, -2.893)	-2.807	(-2.830, -2.785)
θ	0.969	(0.950, 0.986)	-	
σ^2	-		1.020	(1.000, 1.050)

References

Aitkin, A. (1996) A general maximum likelihood analysis of overdispersion in generalized linear models. *Statistics and Computing*, **6**, 251-262.

Athreya, K.B. (1986) Another conjugate family for the normal distribution. *Statistics and Probability Letters*, **4**, 61-64.

Boucher, J.-P. and Denuit, M. (2006) Fixed versus random effects in Poisson regression models for claim counts: a case study with motor insurance. *Astin Bulletin*, **1**, 285-301.

Breslow, N.E. (1984) Extra-Poisson variation in log-linear models. *Journal of the Royal Statistical Society Series C*, **33**, 38-44.

Brooks, S.P. and Gelman, A. (1998) General methods for monitoring convergence of iterative simulations. *Journal of Computational and Graphical Statistics*, **7**, 434-455.

Bureau of Public Roads (1964) *Traffic assignment manual for application with a large, high speed computer.* Washington: U.S. Dept. of Commerce Bureau of Public Roads Office of Planning Urban Planning Division.

Carlson, M. (2002) Assessing microdata disclosure risk using the Poisson-inverse Gaussian distribution. *Statistics in Transition*, **5**, 901-925.

Chen, J.J. and Ahn, H. (1996) Fitting mixed Poisson regression models using quasi–likelihood methods. *Biometrical Journal*, **38**, 81-96.

Chib, S. and Greenberg, E. (1995) Understanding the Metropolis-Hastings algorithm. *The American Statistician*, **49**, 327-335.

Dagpunar, J. (1988) *Principles of Random Variate Generation.* USA: Oxford University Press.

Dean, C., Lawless, J. F. and Willmot, G.E. (1989) A mixed Poisson-inverse-Gaussian regression model. *The Canadian Journal of Statistics*, **17**, 171-181.

Fernández, C., Ley, E. and Steel, M.F.J. (2001) Benchmark priors for Bayesian model averaging. *Journal of Econometrics*, **100**, 381-427.

Font, M., Puig, X. and Ginebra, J. (2013) A Bayesian analysis of frequency count data. *Journal of Statistical Computation and Simulation*, **83**, 229-246.

Gelman, A. (2006) Prior distributions for variance parameters in hierarchical models. *Bayesian Analysis*, **1**, 515-533.

Gelman, A. and Hill, J. (2006) *Data Analysis Using Regression and Multi-level/Hierarchical Models*, 1st edn. New York: Cambridge University Press.

Gelman, A. and Rubin, D.B. (1992) Inference from iterative simulation using multiple sequences. *Statistical Science*, **7**, 457-511.

Hazelton, M.L. (2010) Bayesian inference for network-based models with a linear inverse structure. *Transportation Research Part B*, **44**, 674-685.

Holla, M.S. (1967) On a Poisson-inverse Gaussian distribution. *Metrika*, **11**, 115-121.

Jenelius, E., Petersen, T. and Mattsson, L.G. (2006) Importance and exposure in road network vulnerability analysis. *Transportation Research Part A*, **40**, 537-560.

Jorgensen, B. (1982) Statistical properties of the generalized inverse Gaussian distribution. In *Lecture Notes in Statistics*, vol.9. New York: Springer-Verlag.

Karlis, D. (2001) A general EM approach for maximum likelihood estimation in mixed Poisson regression models. *Statistical Modelling*, **1**, 305-318.

Lawless, J. F. (1987) Negative binomial and mixed Poisson regression. *The Canadian Journal of Statistics*, **15**, 209-225.

Lee, Y. and Nelder, J.A. (1996) Hierarchical generalized linear models (with discussion). *Journal of the Royal Statistical Society Series B*, **58**, 619-678.

Lee, Y. and Nelder, J.A. (2004) Conditional and marginal models: another view. *Statistical Science*, **19**, 219-228.

Martins, T.G. and Rue, H. (2013) Extending INLA to a class of near-Gaussian latent models. arXiv:1210.1434v2.

Medina, A., Taft, N., Salamatian, K., Bhattacharyya, S. and Diot, C. (2002) Traffic matrix estimation. In *Proceedings of the 2002 Conference on Applications, Technologies, Architectures and Protocols for Computer Communications - SIGCOMM '02*, New York: ACM Press.

Meng, X.-L. (1994) Posterior predictive p-values. *The Annals of Statistics*, **22**, 1142-1160.

Nikoloulopoulos, A.K. and Karlis, D. (2008) On modeling count data: a comparison of some well-known discrete distributions. *Journal of Statistical Computation and Simulation*, **78**, 437-457.

Ntzoufras, I. (2009) *Bayesian Modeling Using WinBUGS*, 1st edn. New York: John Wiley and Sons.

Odoki, J.B., Kerali, H.R. and Santorini, F. (2001) An integrated model for quantifying accessibility-benefits in developing countries. *Transportation Research Part A*, **35**, 601-623.

Ortúzar, J. de D. and Willumsen, L.G. (2001) *Modelling Transport*, 3rd edn. Chichester, UK: John Wiley and Sons.

Perrakis, K., Karlis, D., Cools, M., Janssens, D., Vanhoof, K. and Wets, G. (2012a) A Bayesian approach for modeling origin-destination matrices. *Transportation Research Part A*, **46**, 200-212.

Perrakis, K., Cools, M., Karlis, D., Janssens, D., Kochan, B., Bellemans, T. and Wets, G. (2012b) Quantifying input-uncertainty in traffic assignment models. In *91st Annual Meeting of Transportation Research Board*, Washington D.C.: Transportation Research Board.

Puig, X., Ginebra, J. and Perez-Casany, M. (2009) Extended truncated inverse-Gaussian Poisson model. *Statistical Modelling*, **9**, 151-171.

Rue, H., Martino, S. and Chopin, N. (2009) Approximate Bayesian inference for latent Gaussian models by using integrated nested Laplace approximations (with discussion). *Journal of the Royal Statistical Society Series B*, **71**, 319-392.

Shaban, S.A. (1988) Poisson-lognormal distributions. In *Log-normal Distributions: Theory and Applications* (eds E.L. Crow and K. Shimizu), pp. 195-210. New York: Marcel Dekker.

Sohn, K. and Kim, D. (2010) Zonal centrality measures and the neighborhood effect. *Transportation Research Part A*, **44**, 733-744.

Spiegelhalter, D., Thomas, A., Best, N. and Lunn, D. (2003) *WinBUGS User Manual, Version 1.4*. UK: MRC Biostatistics Unit, Institute of Public Health and Department of Epidemiology and Public Health, Imperial College School of Medicine. Available at http://www.mrc-bsu.cam.ac.uk/bugs/winbugs/manual14.pdf

Tebaldi, C. and West, M. (1998) Bayesian inference on network traffic using link count data (with discussion). *Journal of the American Statistical Association*, **93**, 557-576.

Thomas, R. (1991) *Traffic Assignment Techniques*. Aldershot: Avebury Technical.

Wardrop, J. (1952) Some theoretical aspects of road traffic research. *Proceedings of the Institution of Civil Engineers Part II*, **1**, 352-362.

West, M. (1994) Statistical inference for gravity models in transportation flow forecasting. Discussion Paper 94-40, ISDS, Duke University.

Willmot, G.E. (1987) The Poisson-inverse Gaussian distribution as an alternative to the negative binomial. *Scandinavian Actuarial Journal*, **3-4**, 113-127.

Yao, E. and Morikawa, T. (2005) A study of an integrated intercity travel demand model. *Transportation Research Part A*, **39**, 367-381.

Zellner, A. (1986) On assessing prior distributions and Bayesian regression analysis with g-prior distributions. In *Bayesian Inference and Decision Techniques: Essays in Honour of Bruno de Finetti* (eds P. Goel and A. Zellner), pp. 233-243. Amsterdam: North-Holland.